Monthly Notices
of the
ROYAL ASTRONOMICAL SOCIETY

MNRAS **451,** 5153–5157 (2015) doi:10.1093/mnras/stv979

ExoMol molecular line lists – X. The spectrum of sodium hydride

Tom Rivlin,[1] Lorenzo Lodi,[1] Sergei N. Yurchenko,[1] Jonathan Tennyson[1]★ and Robert J. Le Roy[2]

[1]*Department of Physics and Astronomy, University College London, London WC1E 6BT, UK*
[2]*Department of Chemistry, University of Waterloo, Waterloo, Ontario N2L 3G1, Canada*

Accepted 2015 April 30. Received 2015 April 1; in original form 2015 February 21

ABSTRACT

Accurate and complete rotational, rotational-vibrational and rotational-vibrational-electronic line lists are calculated for sodium hydride: both the NaH and NaD isotopologues are considered. These line lists cover all ro-vibrational states of the ground ($X\,^1\Sigma^+$) and first excited ($A\,^1\Sigma^+$) electronic states. The calculations use available spectroscopically-determined potential energy curves and new high-quality, *ab initio* dipole moment curves. Partition functions for both isotopologues are calculated and the effect of quasi-bound states is considered. The resulting line lists are suitable for temperatures up to about 7000 K and are designed for studies of exoplanet atmospheres, brown dwarfs and cool stars. In particular, the NaH $A - X$ band is found to show a broad absorption feature at about 385 nm which should provide a signature for the molecule. All partition functions, lines and transitions are available as supplementary information to this article and at www.exomol.com.

Key words: molecular data – opacity – astronomical data bases: miscellaneous – planets and satellites: atmospheres – stars: low-mass.

1 INTRODUCTION

Although long discussed (Kirby & Dalgarno 1978), the existence of sodium hydride, NaH, is yet to be confirmed in any astronomical bodies. Notably few metal hydrides have been detected in the interstellar medium and searches for NaH in both dense clouds (Plambeck & Erickson 1982) and diffuse clouds (Snow & Smith 1977; Czarny, Felenbok & Roueff 1987) have so far only yielded upper limits. Similarly an attempt to detect the long-wavelength signature for NaH in the atmosphere of Jupiter and Saturn (Weisstein & Serabyn 1996) also proved negative.

While spectroscopic data for long-wavelength studies of NaH has been the subject of the laboratory studies (Leopold et al. 1987; Okabayashi & Tanimoto 2000), and are compiled in the CDMS data base (Müller et al. 2005), the situation is less clear at infrared and visible wavelengths. A recent work on M-dwarf models by Rajpurohit et al. (2013) identified NaH as one of only three molecules for which the necessary spectroscopic data is missing. This is despite the fact that the $A - X$ band of NaH should give an observable feature at visible wavelengths. It is this situation we address here. We note that the next lowest lying singlet electronic excited states of NaH are the $C\,^1\Sigma^+$ (Walji, Sentjens & Roy 2015) and the shallow $B\,^1\Pi$ state (Yang, Zhang & Han 2004) whose yet to be observed spectra lie in the ultraviolet, probably at around 3000 Å.

The large dipole moments of NaH, as well as supposedly making it more amenable to astronomical detection, has also excited the interest of scientists working on ultracold molecules (Juarros et al. 2006; Aymar, Deiglmayr & Dulieu 2009; Su et al. 2010). In particular, it has been suggested that these dipoles should enhance the prospects of molecule formation by radiative association at very low temperatures (Juarros et al. 2006).

The ExoMol project aims to provide line lists of spectroscopic transitions for key molecular species which are likely to be important in the atmospheres of extrasolar planets and cool stars; its aims, scope and methodology have been summarized by Tennyson & Yurchenko (2012). In this paper, ro-vibrational and rovibronic transition lists are computed for the only two stable isotopes of sodium hydride, ^{23}NaH and ^{23}NaD. These line lists consider transitions within and between the two lowest electronic states of NaH, $X\,^1\Sigma^+$ and $A\,^1\Sigma^+$. The resulting line lists are comprehensive and should be valid up to the 7000 K temperature range.

2 METHOD

As with other diatomic systems studied as part of the ExoMol project (Yadin et al. 2012; Barton, Yurchenko & Tennyson 2013; Barton et al. 2014; Yorke et al. 2014; Patrascu, Tennyson & Yurchenko 2015), we treated NaH using both *ab initio* and experimental data. Walji et al. (2015) used a direct potential fit analysis to generate accurate potential energy curves for the ground and first singlet excited states of NaH ($X\,^1\Sigma_g^+$ and 'Avoided Crossing' $A\,^1\Sigma_g^+$). These

★ E-mail: j.tennyson@ucl.ac.uk

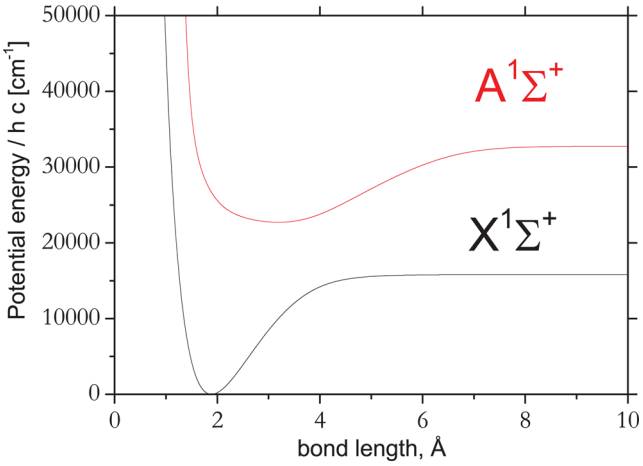

Figure 1. Empirical NaH $X\,^1\Sigma_g^+$ and $A\,^1\Sigma_g^+$ state potential energy curves due to Walji et al. (2015).

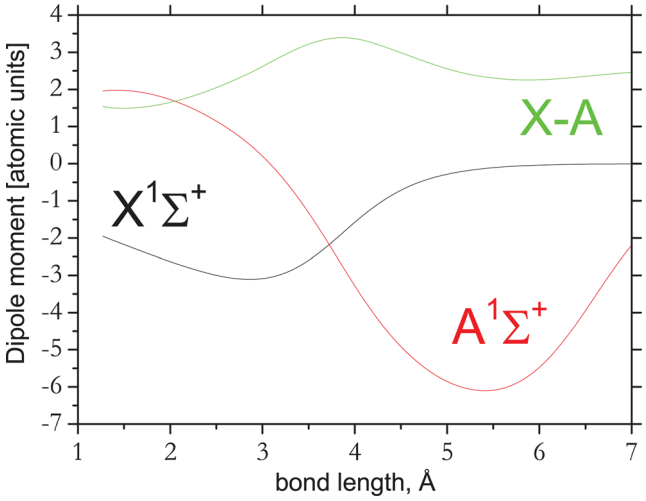

Figure 2. *Ab initio* NaH dipole moment curves as a function of internuclear separation.

curves (also shown in Fig. 1) were then used as input to the program LEVEL version 8.2 (Le Roy 2007) to produce accurate nuclear motion energy levels, wavefunctions and hence transition intensities. A full discussion of how the potential energy curves were derived can be found in Walji et al. (2015), which also gives a comprehensive survey of previous laboratory work on the spectrum of NaH and NaD. We note that the experimental data used by Walji et al. (2015) to determine their curves is insufficient to characterize the last 1000 cm^{-1} of the excited $A\,^1\Sigma_g^+$ below dissociation, where the A state undergoes another avoided crossing (Aymar et al. 2009). The dissociation limit of this state was constrained by the atomic limit neglecting spin–orbit coupling (Walji et al. 2015) and rovibrational states computed in this region must be considered approximate.

2.1 Dipole moments

Ab initio dipole moments were computed on a dense, uniformly-spaced grid of 220 points from r=2.40 to r=13.40 a_0 in steps of 0.05 a_0. Dipoles were computed as expectation value of a multireference configuration interaction (MRCI) calculation using a full valence complete active space model, which distributes the two outer electrons among five orbitals, and the aug-cc-pwCV5Z basis set. Orbitals were produced using a state-averaged complete active space self-consistent field which considered both the X and A states. The core 2s2p electrons were correlated at the MRCI stage. A single run takes about 4 min.

Fig. 2 shows our two diagonal dipole moment curves and the off-diagonal A–X transition moment. The diagonal dipoles have a somewhat unusual shape which is undoubtedly associated with the changing character of the NaH wavefunction as a function of geometry. The dipole moment of ground state NaH has been determined experimentally (Dagdigian 1979), but not particularly accurately. Conversely there have been quite a number of theoretical studies on the problem. The most recent is a comprehensive calculation of all three moments considered here by Aymar et al. (2009), who also provide a comprehensive survey of the previous literature. Our results are in excellent agreement with those of Aymar et al. (2009), who also find the various turning points in the dipole curves which are a feature of our calculations.

Our dipole moment points, which are provided in the supplementary material, were input directly into LEVEL.

3 RESULTS

3.1 Partition function

Partition functions for NaH and NaD were calculated by summing over all energy levels calculated. Szidarovszky & Császár (2015) have recently shown that inclusion of quasi-bound (resonance or pre-dissociative) states can influence the partition function sums at higher temperatures. Here, we present partition functions for both NaH and NaD obtained by summing both over all the truly bound states of the system and also by including quasi-bound states determined using LEVEL. Table 1 compares these two methods and suggests that below 2000 K, the influence of quasi-bound states on the partition sum can safely be neglected. Above this temperature the quasi-bound states have a small but increasing influence. However for consistency with our previous work and because we do not consider transitions to quasi-bound states, we ignore the effect of quasi-bound states below. For high-accuracy work at higher temperatures this approximation may need to be re-visited.

Table 1 also compares our NaH partition functions with those of Sauval & Tatum (1984) and the CDMS data base (Müller et al. 2005). Our results cover a larger temperature range: CDMS values only go up to 300 K for NaH, and Sauval & Tatum only claim their values are accurate for 1000–9000 K. The latter values were multiplied by the factor 8 in order to explicitly account for the nuclear spin degeneracy in accord with the HITRAN (Fischer et al. 2003) convention, used by ExoMol; the CDMS partition function had to be multiplied by 2. According to the convention of CDMS, the common factors in partition functions are usually divided to keep them small (Müller et al. 2005). After these adjustments results give good agreement with Sauval & Tatum and CDMS in the appropriate temperature ranges, although there is a slight divergence from Sauval & Tatum's values at higher temperature ranges.

A polynomial fit of this work's partition functions is given in Table 2. The values in Table 2 are coefficients in the following equation:

$$\log_{10} Q(T) = \sum_{n=0}^{8} a_n (\log_{10} T)^n, \quad (1)$$

which was based on a series expansion used by Vidler & Tennyson (2000).

Table 1. Partition function of NaH compared with other sources.

T(K)	This work (with quasi-bound)	This work (without quasi-bound)	Sauval & Tatum (1984)	CDMS
37.5			51.00	45.93
38	46.50	46.50	51.67	
75	89.10	89.10	97.98	89.10
150	175.73	175.73	182.99	175.72
225	262.83	262.83	266.93	262.62
300	351.39	351.39	353.94	349.79
500	607.74	607.74	610.87	
1000	1479.85	1479.85	1460.52	
1500	2764.91	2764.89	2668.35	
2000	4521.88	4520.67	4303.28	
2500	6811.55	6799.15	6437.62	
3000	9692.63	9633.66	9149.42	
3500	13 205.11	13 024.25	12 523.04	
4000	17 363.28	16 941.48	16 649.49	
4500	22 161.35	21 341.29	21 626.79	
5000	27 583.33	26 178.70	27 560.23	
5500	33 610.90	31 415.33	34 562.72	
6000	40 227.09	37 021.39	42 755.06	

Table 2. Fitting parameters for the partition function of NaH/NaD. Fits are valid for temperatures up to 9000 K within 1 per cent.

	NaH (with quasi-bound)	NaH (without quasi-bound)	NaD (with quasi-bound)	NaD (without quasi-bound)
a_0	5.203 127 197 99	−0.192 307 354 79	−1.611 662 914 73	−0.192 307 354 79
a_1	−19.012 610 246 30	3.708 598 733 34	9.532 817 631 05	3.708 598 733 34
a_2	34.832 553 672 50	−3.078 873 325 29	−13.183 957 042 40	−3.078 873 325 29
a_3	−34.374 634 167 70	0.719 238 662 64	10.406 622 258 70	0.719 238 662 64
a_4	20.730 519 609 60	1.119 295 409 33	−4.495 784 538 50	1.119 295 409 33
a_5	−7.760 512 520 85	−0.999 028 835 69	1.016 744 029 73	−0.999 028 835 69
a_6	1.751 968 122 28	0.347 067 333 27	−0.090 687 521 70	0.347 067 333 27
a_7	−0.217 345 374 82	−0.056 128 847 04	−0.003 559 804 20	−0.056 128 847 04
a_8	0.011 340 935 77	0.003 488 757 07	0.000 817 890 72	0.003 488 757 07

Table 3. Summary of the computed NaH and NaD line lists.

	NaH X state	NaH A state	NaD X state	NaD A state
Maximum v	21	32	30	34
Maximum J	81	123	113	171

3.2 Line lists

Line lists were calculated for the two main isotopologues: NaH and NaD. All transitions satisfying the selection rule $\Delta J = \pm 1$ between all ro-vibrational states in the electronic ground state and first electronically-excited state were considered. A summary of each line list is given in Table 3. Although every possible transition was computed, some were very weak and are not included in the final line list.

4 APPLICATIONS

The line lists contain hundreds of thousands of transitions. They are separated into separate energy levels and transitions files. This is done using the standard ExoMol format (Tennyson, Hill & Yurchenko 2013) where the states file gives all energy levels and associated quantum numbers, and the transitions file gives Einstein A coefficients and the numbers of the associated states. Extracts from the start of the NaH states and transitions files are given in Tables 4 and 5. The full line list can be downloaded from the ExoMol website www.exomol.com or from the VizieR service from the website of the Strasbourg Data Center cds.u-strasbg.fr. A small computer program which uses these files to compute spectra is given in the supplementary material to Yorke et al. (2014).

The direct potential fit Walji et al. (2015) essentially reproduced all experimental data within its stated uncertainty once a very modest amount of data cleaning had been performed.

Dagdigian (1976), Baltayan, Jourdan & Nedelec (1976) and Nedelec & Giroud (1983) measured radiative lifetimes for a number of A-state ro-vibrational levels. These measurements suggest that the lifetime actually has little dependence on the actual level involved with a sudden increase for $v = 21$. A comparison with our predictions for some of these states is listed in Table 6: in general the agreement is very good. However, in contrast to Nedelec & Giroud (1983), we observe the increase of the lifetime of the A-state levels at lower vibrational excitations than $v = 21$. The increase is associated with the X-state dissociation threshold of 15 797.4 cm^{-1}, which truncates the contributions from the bound states of the ground electronic state. Thus, the lower experimental

Table 4. Extract from the states file for NaH. The zero of energy is taken to be the energy of the lowest energy level. The files contain 3339 levels for NaH and 5960 levels for NaD.

n	$\tilde{E}$	g	J	State	v
1	0.000 000	8	0.0	X	0
2	1133.102 453	8	0.0	X	1
3	2228.214 399	8	0.0	X	2
4	3285.975 269	8	0.0	X	3
5	4306.940 010	8	0.0	X	4
6	5291.562 054	8	0.0	X	5
7	6240.146 564	8	0.0	X	6
8	7152.840 057	8	0.0	X	7
9	8029.619 734	8	0.0	X	8
10	8870.226 718	8	0.0	X	9
11	9674.057 941	8	0.0	X	10
12	10 440.079 797	8	0.0	X	11

Notes. n: state counting number.
$\tilde{E}$: state energy in cm^{-1}.
g: state degeneracy.
J: state rotational quantum number.
v: state vibrational quantum number.
State: electronic state label.

Table 5. Extract from the.trans file for NaH. Full tables are available from the ExoMol website www.exomol.com or from the VizieR service from the website of the Strasbourg Data Center cds.u-strasbg.fr. The files contain 79 898 transitions for NaH and 167 224 transitions for NaD.

f	i	A_{if}
342	322	2.1771E+01
3190	3198	5.9304E+00
1168	1200	6.8873E−01
3329	3327	1.1725E+02
477	495	5.0419E−01
3225	3217	8.4415E+01
2887	2870	3.5561E+01
929	938	1.0760E−01
759	744	1.1033E+01
3286	3280	9.6810E+01

Notes. f: final state number.
i: initial state number.
A_{if}: Einstein A coefficient in s^{-1}.

Table 6. Lifetimes (in ns) of selected ro-vibrational states within the $A\,^1\Sigma^+$ electronic state: comparison of experiment Dagdigian (1976); Nedelec & Giroud (1983) and calculated (this work).

v'	J'	Ref.	Exp.	Calc.
3	8	Dagdigian (1976)	24.0 (3)	25.71
4	11	Dagdigian (1976)	28.3 (3)	25.69
5	16	Dagdigian (1976)	27.1 (3)	26.44
3	4	Nedelec & Giroud (1983)	27	25.37
4	6	Nedelec & Giroud (1983)	28.5	25.16
7	6	Nedelec & Giroud (1983)	26.5	25.40
9	6	Nedelec & Giroud (1983)	26	29.71
11	6	Nedelec & Giroud (1983)	25.5	33.10
14	7	Nedelec & Giroud (1983)	27	36.49
18	11	Nedelec & Giroud (1983)	27.5	44.01
21	6	Nedelec & Giroud (1983)	35	48.67

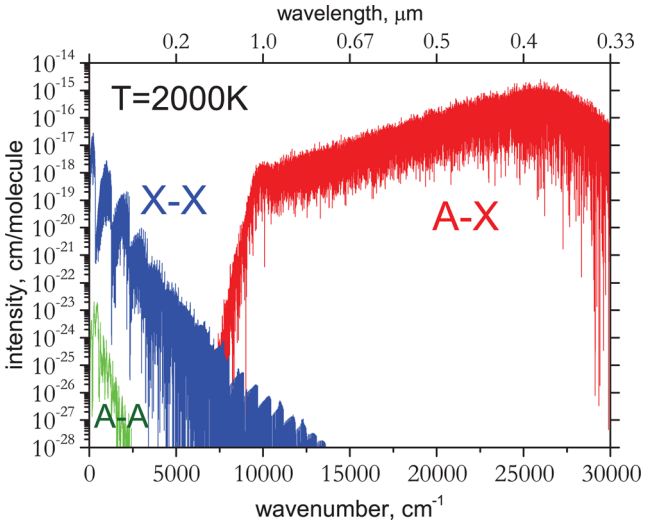

Figure 3. Overview of the X–X, A–A, and A–X absorption spectrum of ^{23}NaH at 2000 K. The theoretical spectrum is convolved with a Gaussian profile with a half-width half-maximum (HWHM) of 0.1 cm^{-1}.

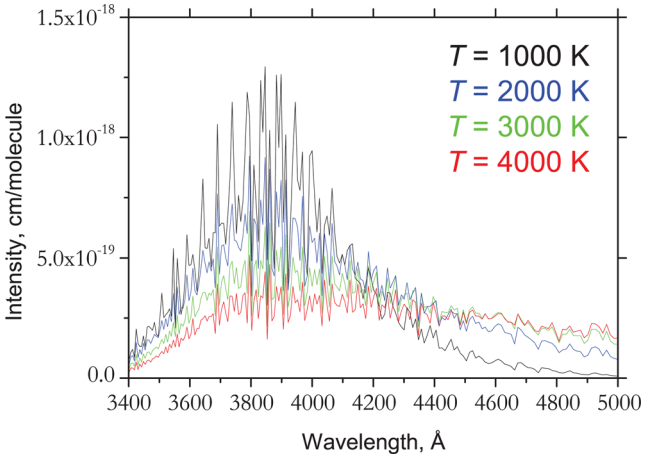

Figure 4. Computed A–X absorption spectrum of ^{23}NaH at different temperatures. A Doppler profile was used to convolve the theoretical spectrum. Wavenumber bin of 50 cm^{-1} was chosen to mimic resolving power of about 500–1000.

values of the lifetimes can be attributed to the transitions to the $X\,^1\Sigma^+$ quasi-bound states, which are not included in our line lists.

Fig. 3 gives an overview of the entire spectral range covering the X and A systems, from infrared to visible shown as an absorption spectrum generated for $T = 2000$ K. Of particular astronomical interest is likely to be the $A - X$ band in the 380 nm region. The $A - X$ band does not exhibit sharp features which can be attributed to the shallow A potential energy curve, see Fig. 1. This reduces the chances of NaH to be detected at visible wavelengths, especially at high temperature, as also illustrated by Fig. 4, where the $A - X$ absorption band is shown for a set of temperatures from 1000 to 4000 K.

Fig. 5 shows the pure rotational band of NaH at $T = 298$ K compared to the spectra from the CDMS data base. The latter was generated by averaging over the hyperfine lines, which are not resolved in our line lists. The agreement between intensities can be attributed to the equilibrium X-state dipole moment value of 6.7 D

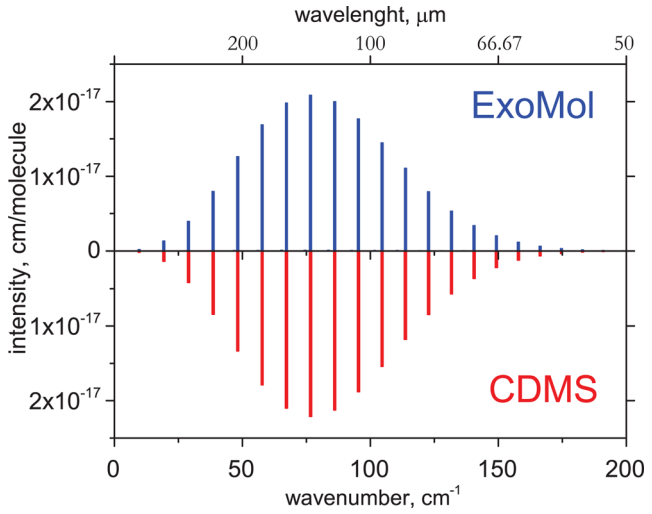

Figure 5. Rotational spectrum of ^{23}NaH computed at $T = 298$ K: ExoMol (current work) and CDMS (Müller et al. 2005). The CDMS intensities were obtained by summing individual hyperfine transitions; these were generated by Müller et al. (2005) using an equilibrium dipole moment of 6.7 D as calculated by Sachs et al. (1975).

of Sachs, Hinze & Sabelli (1975) used by CDMS. Our value is 6.43 D at $r_e = 1.887$.

5 CONCLUSIONS

We present comprehensive line lists for NaH and NaD. These are based on the direct solution of the nuclear motion Schrödinger equation using potential energy curves obtained by fitting to experimental data of measured transitions, all calculated by Walji et al. (2015). These were combined with a new *ab initio* dipole moment curve to produce comprehensive line lists for these two species. The strong *A*–*X* feature about 380 nm should provide a signature for NaH in the atmospheres of cool stars, brown dwarfs and exoplanets. However, the shallow nature of the upper $A\ ^1\Sigma^+$ electronic state means that this feature is predicted to be rather broad. While this means that NaH can make a significant contribution to the opacity, it is likely to make this feature difficult to detect.

NaH and AlH were recently identified as key diatomic species whose spectral data was completely missing from M-dwarf models (Rajpurohit et al. 2013). A study on AlH has just been completed and will be reported soon.

ACKNOWLEDGEMENTS

This work was supported by the ERC under the Advanced Investigator Project 267219 and a Wolfson Royal Society Research Merit award.

REFERENCES

Aymar M., Deiglmayr J., Dulieu O., 2009, Can. J. Phys., 87, 543
Baltayan P., Jourdan A., Nedelec O., 1976, Phys. Lett. A, 58, 443
Barton E. J., Yurchenko S. N., Tennyson J., 2013, MNRAS, 434, 1469
Barton E. J., Chiu C., Golpayegani S., Yurchenko S. N., Tennyson J., Frohman D. J., Bernath P. F., 2014, MNRAS, 442, 1821
Czarny J., Felenbok P., Roueff E., 1987, A&A, 188, 155
Dagdigian P. J., 1976, J. Chem. Phys., 64, 2609
Dagdigian P. J., 1979, J. Chem. Phys., 71, 2328
Fischer J., Gamache R. R., Goldman A., Rothman L. S., Perrin A., 2003, J. Quant. Spectrosc. Radiat. Transfer, 82, 401
Juarros E., Pellegrini P., Kirby K., Cote R., 2006, Phys. Rev. A, 73, 041403
Kirby K., Dalgarno A., 1978, ApJ, 224, 444
Le Roy R. J., 2007, LEVEL 8.0 A Computer Program for Solving the Radial Schrödinger Equation for Bound and Quasibound Levels. University of Waterloo Chemical Physics Research Report CP-663. Available at: http://leroy.uwaterloo.ca/programs/
Leopold K. R., Zink L. R., Evenson K. M., Jennings D. A., 1987, J. Mol. Spectrosc., 122, 150
Müller H. S. P., Schlöder F., Stutzki J., Winnewisser G., 2005, J. Mol. Struct., 742, 215
Nedelec O., Giroud M., 1983, J. Chem. Phys., 79, 2121
Okabayashi T., Tanimoto M., 2000, ApJ, 543, 275
Patrascu A. T., Tennyson J., Yurchenko S. N., 2015, MNRAS, 449, 3613
Plambeck R. L., Erickson N. R., 1982, ApJ, 262, 606
Rajpurohit A. S., Reyle C., Allard F., Homeier D., Schultheis M., Bessell M. S., Robin A. C., 2013, A&A, 556, A15
Sachs E. S., Hinze J., Sabelli N. H., 1975, J. Chem. Phys., 62, 3367
Sauval A. J., Tatum J. B., 1984, ApJS, 56, 193
Snow T. P., Smith W. H., 1977, ApJ, 217, 68
Su Q., Yu J., Niu Y., Cong S., 2010, Chem. Phys. Lett., 27, 3401
Szidarovszky T., Császár A. G., 2015, J. Chem. Phys., 142, 014103
Tennyson J., Yurchenko S. N., 2012, MNRAS, 425, 21
Tennyson J., Hill C., Yurchenko S. N., 2013, in Gillaspy J. D., Wiese W. L., Podpaly Y. A., eds, AIP Conf. Proc. Vol. 1545, Eighth International Conference on Atomic and Molecular Data and their Applications: ICAMDATA-2012. Am. Inst. Phys., New York, p. 186
Vidler M., Tennyson J., 2000, J. Chem. Phys., 113, 9766
Walji S.-D., Sentjens K., Roy R. J. L., 2015, J. Chem. Phys., 142, 044305
Weisstein E. W., Serabyn E., 1996, Icarus, 123, 23
Yadin B., Vaness T., Conti P., Hill C., Yurchenko S. N., Tennyson J., 2012, MNRAS, 425, 34
Yang C. L., Zhang X., Han K. L., 2004, J. Mol. Struct., 676, 209
Yorke L., Yurchenko S. N., Lodi L., Tennyson J., 2014, MNRAS, 445, 1383

SUPPORTING INFORMATION

Additional Supporting Information may be found in the online version of this article:

Table 4. Extract from the states file for NaH.
Table 5. Extract from the.trans file for NaH.
(http://mnras.oxfordjournals.org/lookup/suppl/doi:10.1093/mnras/stv979/-/DC1).

Please note: Oxford University Press are not responsible for the content or functionality of any supporting materials supplied by the authors. Any queries (other than missing material) should be directed to the corresponding author for the article.

This paper has been typeset from a TEX/LATEX file prepared by the author.